September 25th - 28th, 2017
NTERFACES
architecture . engineering . science IASS 2017 hamburg

Proceedings of the IASS Annual Symposium 2017
"Interfaces: architecture . engineering . science"
September 25 - 28th, 2017, Hamburg, Germany
Annette Bögle, Manfred Grohmann (eds.)

A Minimal Surface Membrane Sculpture

Ruy Marcelo O. PAULETTI*, Sigrid ADRIAENSSENS[a], Alexander NIEWIAROWSKI[a] , Victor CHARPENTIER[a], Max COAR[a], Tracy HUYNH[a], Xi LI[a]

*Polytechnic School at the University of São Paulo
Av. Prof. Almeida Prado, Trav. 2, 83 – 05508-900, São Paulo, SP, Brazil
pauletti@usp.br

[a] Department of Civil and Environmental Engineering
Princeton University, Princeton, NJ, 08540, USA

Abstract

This paper presents the design, analysis, and fabrication of a membrane sculpture based on the Costa minimal surface. The work was developed during the Spring of 2016 at Princeton University as a pedagogical exercise combining the mathematics of minimal shapes with the major aspects of membrane structure design. Three different numerical form finding methods were employed independently to obtain a genus 2 Costa-Hoffman-Meeks minimal surface, which was subsequently fashioned into a unique and elegant art object. In the fabrication process, the 3D surface was first subdivided considering its inherent symmetries, resulting in three unique pattern shapes that were flattened, cut out from fabric, and finally sewn together. A bending-active tensioning system was designed and fabricated from initially straight fiberglass rods and custom 3D-printed connections. Although Costa surface has inspired at least a previous art installation and a membrane roof, the current sculpture innovates in the use of a bending-active support system, which renders the system self-supported, with remarkable adherence to the prescribed geometric parameters, yielding a smooth and well-stretched fabric surface, and providing a successful academic example of interface between art, engineering and science.

Keywords: Fabric sculpture, membrane structure, minimal surface, Costa surface, non-linear analysis, bending-active, fabrication and design

1. Introduction

The study of minimal surfaces, characterized by the property of a minimal area within a fixed boundary, is important from both theoretical and practical point of views. They are also the solution geometry for a membrane constrained to that same boundary under an isotropic and uniform plane stress field (Eisenhart 1909 [9], Douglas 1931 [8], Isenberg 1978 [12]). These properties render minimal surfaces an interesting design option for membrane structures, since they are uniquely defined, for a given boundary, and provide economy of material and more regular fabric patterns.

Minimal surfaces have also attracted the interest of scientists since the times of Lagrange (who solved the problem for some surfaces of the type) and Euler (who proved that minimal surfaces have zero-mean curvature everywhere, and therefore are either plane or anticlastic). In the nineteenth century, the Belgian physicist Joseph Plateau showed that analogue solutions to area minimization problems could be produced by dipping wire frameworks into a bath of soap solution.

Less frequently studied are the evident sculptural qualities of minimal surfaces, such as double curvature, continuity, and intrinsic lightness. Although minimal surfaces have inspired many art works, their physical representations often contradict these qualities by using stiff and heavy materials, or rough

finishes. Soap films successfully represent minimal surfaces, but their ephemeral nature does not permit long term exhibition. On the other hand, tension structures are both durable and express purity of form. There is little hidden in a prestressed membrane, which serves both as structure and the definition of form.

Among the known minimal surfaces, the Costa surface is particularly interesting for its simplicity from afar and intricacy upon closer inspection. This paper explores a rendition of the Costa Surface as a tensile structure, and shows how mathematics can create inspiring forms. The Costa minimal surface was discovered by then-graduate student Celso de Jose Costa at the University of Brazil in 1982. He described in his doctoral dissertation (Costa 1982 [5]) a surface that, from afar, appeared as a catenoid radially bisected by a plane (or at least it would appear so a decade later when computers had advanced sufficiently to accurately portray this shape). However, closely observing, it can be seen that there is no intersection at all, and instead the "plane" flows smoothly around handles (holes in a surface) to join the catenoid. Costa's discovery shattered a 200-year old conjecture that the plane, the helicoid, and the catenoid were the only topologically finite, complete, embedded minimal surfaces. Since the publication of Costa's doctoral dissertation, research on embedded minimal surfaces has exploded and the surface was generalized for higher genus orders by (Hoffman and Meeks 1990 [10]). However, the original genus 1 version of the form remains the symbol of the research area.

The first computer rendering of the surface was done by David Hoffman at University of Massachusetts at Amherst with help of programmer James Hoffman in 1985 [11]. Afterwards, a limited number of artistic or architectural renditions of a Costa surface have been created. The sculptor Helaman Ferguson and his team built some large snow (1999) and stone (2008) Costa surfaces. On an architectural scale, the Australian Wildlife Health Center by MvS Architects (2006) features a tensile roof inspired by the form. To the best of the authors' knowledge, this is the first tensile membrane manifestation of a Costa surface, followed only by an installation by Pauletti, first displayed at the University of São Paulo, in 2008, and later at the *Universidad de la Republica*, Montevideo, in 2011.

This paper reports the collaborative work developed during the Spring of 2016 at Princeton University by the students enrolled at the graduate course CEE540, to combine the mathematics of minimal shapes with the major aspects of membrane structure design and production. The overall size, geometry, materials and production methods were all defined by the students, seeking an object that required a sophisticated production, and capable of attracting bystanders' curiosity.

2. Form finding

The Costa surface is a topologically finite, complete, embedded surface (Hoffman and Meeks III 1985 [11], Hoffman and Meeks 1990 [10], Meeks III and Pérez 2011 [14]). "Topologically finite" means that the surface can be made by puncturing a compact surface. In this case, a torus is punctured 3 times, and the surface is stretched to achieve the form. "Complete" means the surface has no boundary. The Costa surface is usually rendered as being cropped by an arbitrary enclosing surface, resulting in three "boundary rings," while the surface continues asymptotically approaching an infinite plane and a catenoid. An "embedded" surface has no self-intersections.

In this project, a generalized Costa surface with 6 holes (more specifically, a Costa-Hoffman-Meeks surface of genus 2) was chosen, since it allowed for the introduction of a stable, bending-active support system. The sculpture's dimensions were predefined by prescribing the relative positions and sizes of the three boundary rings. The top and bottom rings were given a diameter of 1.5 m, and the middle ring a diameter of 2 m. The height of the membrane structure was set to be 1.5 m. A rough mesh (with 2821 nodes and 5460 triangular membrane elements) that satisfies the boundary geometry and topological requirements mentioned above was created with Grasshopper (Figure 1), and then the associated minimum surface was sought by different numerical methods.

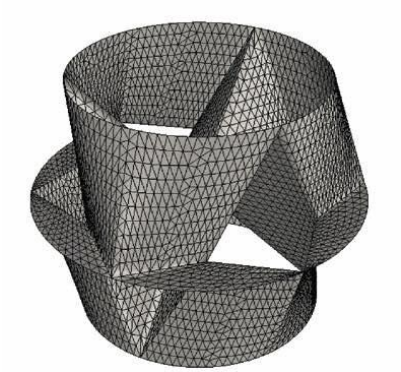

Figure 1: Initial mesh in perspective view

2.1. Numerical Methods for Form Finding

While it is possible to define the form of a Costa surface analytically, the authors used numerical methods instead. Two different approaches were used to find the required minimal surface. The first approach deals with an exclusively geometrical area minimization problem, which is solved using the dynamic relaxation method (DRM). The second approach relies on the analogy between minimal surfaces and soap films. The resulting non-linear mechanical equilibrium problem was solved by the standard Newton-Raphson method (NRM), as well as by the Natural Force Density Method (NFDM). In all, these two approaches yield three numerical methods that were independently applied, and the results were compared.

2.1.1. Direct Area Minimization solved using the Dynamic Relaxation Method

The necessary 1st order condition for the area of a surface spanned by a configuration vector $\mathbf{x} = \mathbf{x}^r + \mathbf{u}$ to be an extremum is given by the non-linear equation

$$\mathbf{p}\left(\mathbf{u}^*\right) = \left.\frac{\partial A}{\partial \mathbf{u}}\right|_{\mathbf{u}^*} = \mathbf{0} \tag{1}$$

where A is the surface area and $\mathbf{u}$ is a displacement vector field, with respect to a reference configuration $\mathbf{x}^r$. Prescribed boundaries are imposed by the equality restriction $\mathbf{x}_P - \bar{\mathbf{x}}_P = \mathbf{0}, \forall P \in C$, where C is the prescribed boundary curve, $\bar{\mathbf{x}}_P$ is a vector spanning the prescribed coordinates and $\mathbf{p}(\mathbf{u})$ may be understood as a generalized internal load vector. That this extremum is a minimum can be verified *ad hoc* (Souza 2008 [22]).

Analytical solution of the nonlinear Eq. (1)may be rather difficult for complex boundary geometries, leaving numerical solution such as the popular Newton-Raphson method (NRM) as the only general way to tackle the problem. In NRM the solution $\mathbf{u}^*$ is sought starting from an initial estimative $\mathbf{u}_0$ and iterating the recurrence formula $\mathbf{u}_{i+1} = \mathbf{u}_i - \mathbf{H}_i^{-1}\mathbf{p}_i$, where the Hessian matrix is defined as $\mathbf{H} = \frac{\partial \mathbf{p}}{\partial \mathbf{u}}$. However, it is intuitive to realize that the area of any smooth surface with fixed boundaries is indifferent to deformations involving infinitesimal displacements tangent to the surface itself. This is reflected in the fact that the Hessian matrix becomes more and more ill-conditioned, as any algebraic solution of Eq. (1) is approached. In practice, this characteristic overrules the direct solution of Eq. (1) by means of pure NRM. Because of this restriction in solving the problem of direct area minimization, NRM is usually replaced by other algorithms that avoid the exact inversion of the Hessian matrix, such as conjugate gradient methods (Souza 2008 [22]) or the BFGS algorithm (Arcaro and Klinka 2009 [2]), which are capable of converging to one of the infinite solutions that exist for any given mesh topology.

In this work, the dynamic relaxation method (DRM) was chosen due to its ubiquity in the field of tensile structure design.

DRM offers an interesting alternative to solve complicated nonlinear equilibrium problems, replacing the static equilibrium problem by a pseudo-dynamic analysis, where fictitious masses and damping matrices are arbitrarily chosen to control the stability of the time integration process (Day 1965 [7], Otter 1965 [15], Barnes 1975 [4]). Thus, instead of solving Eq. (1), we follow the damped vibrations of the dynamic system $\mathbf{M}\ddot{\mathbf{u}} + \mathbf{C}\dot{\mathbf{u}} + \mathbf{p}(\mathbf{u}) = \mathbf{0}$, until it comes to a rest, at a solution of Eq. (1). Usually, damping coefficients close to the system's critical damping are chosen, to speed up the convergence to the static equilibrium configuration. Moreover, since the mass and damping matrices are fictitious, they may be adjusted to keep the time-increments small enough to guarantee stability, but as large as possible to reduce the number of steps required for convergence to the static solution. Applied to the direct area minimization problem, the external vector, the damping matrix, and the mass matrix are generalized quantities with dimensions of [m], [s], and [s^2], respectively. Furthermore, a popular technique associated with DRM, called kinetic damping (Cundall 1976 [6]) is to disregard the damping term altogether and arbitrarily zero the nodal velocities whenever a peak of generalized kinetic energy is detected.

2.1.2. Soap Film Analogy solved using Newton-Raphson and the Natural Force Density Method

It can be shown that the geometry associated with the equilibrium of an isotropic and uniform stress field is also the geometry that minimizes the area for that geometry. This notion, also known as the *soap film analogy*, can be traced back to the physicist J.A.F Plateau (1873 [20]) but has only been proved much more recently by Almgren and Taylor (1976 [1]). The soap film analogy provides a practical way to recast the problem of area minimization as a problem of membrane equilibrium under a prescribed stress field. DRM could also be used in this approach, but in this work, two alternative methods were selected as described below. The imposition of positive initial stress fields guarantees geometrical stiffness in the direction normal to the surface, while the definition of some elastic properties to the membrane guarantees stiffness in the tangential direction. Combined, these effects overcome the ill-conditioning of the Hessian matrix discussed above, permitting the application of NRM. Starting from an arbitrary initial geometry, onto which a uniform and isotropic stress field is imposed, a viable equilibrium configuration is obtained, with a generally non-uniform stress field. The process is then repeated with the previous viable geometry assumed as a new initial one, but reimposing the original stress field, until convergence of both geometry and stresses is achieved.

An alternative method for finding equilibrium configurations of membrane structures that avoids the problems related to nonlinear analysis is the Natural Force Density Method (NFDM), an extension of the well-known Force Density Method (Linkwitz 1971 [13], Schek 1974 [21]). NFDM was first suggested by Pauletti in 2006 [16], based on the natural approach introduced by Argyris for the Finite Element Method (Argyris, Dunne et al. 1974 [3]). In this method, the prescribed initial stress field $\boldsymbol{\sigma}$ in triangular elements is converted into quantities called natural force densities, according to $\mathbf{n} = [n_1 \quad n_2 \quad n_3] = V\boldsymbol{\mathcal{L}}^{-2}\mathbf{T}^{-T}\boldsymbol{\sigma}$, where V is the element volume, $\boldsymbol{\mathcal{L}} = diag\{\ell_1 \quad \ell_2 \quad \ell_3\}$ collects the element side lengths, and $\mathbf{T}$ is a stress transformation matrix. It can be shown that the imposition of natural force densities linearizes the membrane equilibrium problem (Pauletti 2006 [16], Pauletti and Pimenta 2008 [18], Pauletti 2011 [19]). If the NFDM is applied iteratively, re-imposing a uniform and isotropic stress field to the shape resulting at every iteration, the method will again converge to a minimum surface, through the solution of a series of linear systems. This is a clear advantage, if compared to NRM, which also converges to minimal configurations, but requires the solution of non-linear systems at every iteration.

2.3. Results and Discussion

Solutions for the minimal Costa surface, considering the three numerical approaches outlined above were obtained using a previously implemented MATLAB program named SATS (System for the Analysis of Taut Structures) (Pauletti 2008 [17]) with minor adaptations. All three approaches started with the same initial mesh generated in Grasshopper (Figure 1).

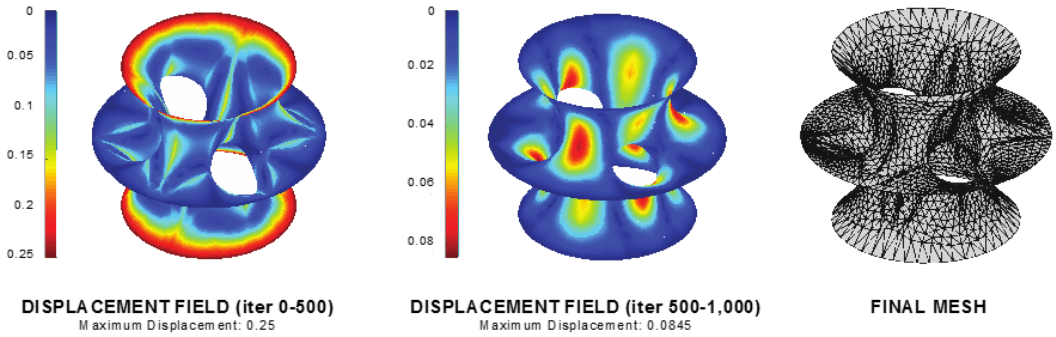

(a) (b) (c)

Figure 2: Direct area minimization using DRM: (a) Intermediate geometry showing the norm of displacements relative to the initial geometry, (b) Final geometry showing the norm of displacements relative to the intermediate geometry, (c) Final mesh with visible element distortion

Figure 2 shows the results obtained for the area minimization problem using DRM. The calculation process took 1000 iterations with the geometry being updated after 500 iterations to speed up convergence. It can be observed from the final mesh configuration that a smooth geometry is achieved, but with significant element distortions, reflecting the fact the nodes are unconstrained in the tangential direction. These distortions correspond to the creases in the initially non-smooth geometry, which give rise to high unbalanced load vectors. In principle, distortion could be prevented by adding some artificial stiffness in the tangential direction, but that would mar the purely geometrical approach originally intended. In that case, a full mechanical analogy (discussed below) is preferred.

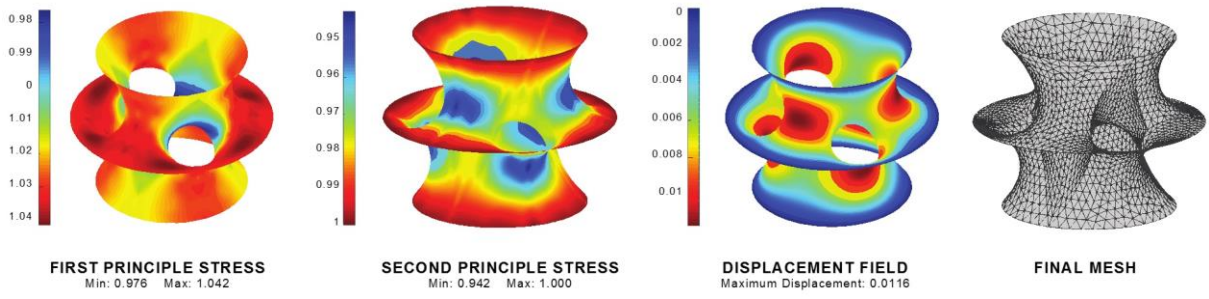

(a) (b) (c) (d)

Figure 3: Solving soap-film analogy with NRM: (a/b) First and second principle stresses at final configuration. (c) Displacements from penultimate to final configurations. (d) Final mesh geometry

Figure 3 shows the results obtained considering the soap film analogy solved by NRM: Multiple rounds of non-linear equilibrium analyses were performed, while reducing the error limits. After convergence for each round of calculations, the geometry was updated, adding up the obtained displacements and the original stress field was reimposed. The displacements between consecutive analyses gradually decreased. The final equilibrium configuration was reached after four rounds of non-linear equilibrium analyses, with a total of 22 iterations and a maximum displacement norm of less than 10^{-5} m between the penultimate and ultimate configurations. In the plotting of the stresses, it is seen that uniform

maximum and minimum principle stress fields were obtained with small deviations between the two values, also indicating a fairly isotropic stress state. That means that the final surface is indeed minimal, within a numerical tolerance.

Finally, Figure 4 shows the results obtained considering the soap film analogy solved by NFDM. As previously discussed, NFDM provides viable equilibrium configurations at every iteration, generally resulting in non-uniform stress fields. However, as for NRM, updating the geometry and reimposing the stresses allowed NFDM to converge to the minimal shape after only five rounds. Once again, the minimality of the surface can be verified by the uniformity and small variations between the first and second principle stress fields. In this case, displacements were not plotted since NFDM is formulated in terms of global coordinates.

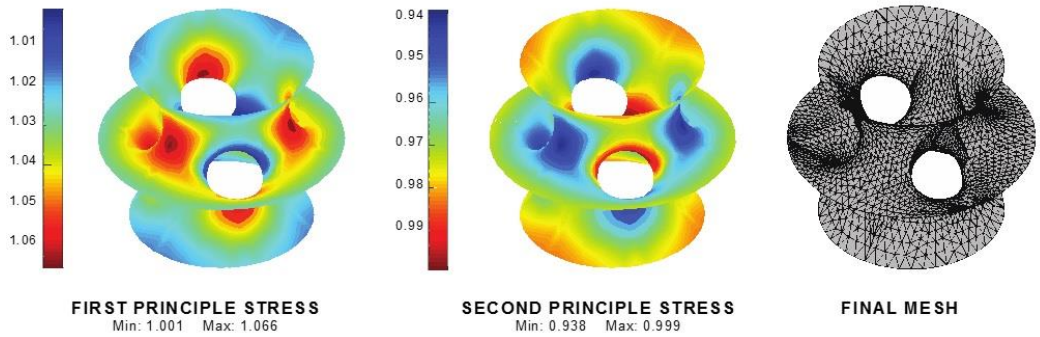

(a) (b) (c)

Figure 4: Solving soap-film analogy with NFDM: (a/b) First and second principle stresses at final configuration. (c) Final mesh geometry

Table 1 compares the total surface area obtained with each of the three numerical methods, as well as the number of iterations required for convergence. The three methods effectively reduced the surface area of the initial mesh under the given boundary conditions, and created suitable final configurations that are close to the actual minimal surface, as can be concluded by inspection of the resulting stresses, displacements, and total areas. DRM required by far the largest number of iterations and was prone to severe mesh distortion. However, it is capable of solving the direct area minimization problem, something that cannot be achieved with pure NRM. As per the two-strategies used to solve the soap-film analogy, both NRM and NFDM showed good convergence, with NFDM being considerably faster.

Table 1: Form finding results summary (Area of initial mesh: 10.49 m^2)

Method	Surface area at convergence (m^2)	Iterations
Direct area minimization	8.25	1000
Newton-Raphson Method	8.28	22
Natural Force Density Method	8.25	5

3. Manufacturing and assembly

The manufacturing of membrane structures is a relatively complex undertaking because they are usually characterized by double curvature, but produced from planar fabrics. The 3D surface must be subdivided into adequate patterns, and these patterns should be flattened. There is always an intrinsic error introduced by this process, which can only be minimized by increasing the subdivision. When working with architectural fabrics, which are characterized by relatively high stiffness, this error may introduce visible slackness or wrinkles if not properly managed. However, more flexible fabrics allow for a cruder patterning. The current work takes profit of the flexibility of the selected material in order produce a Costa surface sculpture with only three different patterns that reflect its internal symmetries (Figure 5).

3.1. Pattern Finding and Optimization

The final mesh obtained by NFDM was selected as the basis for patterning because it yielded the most regular mesh. The internally straight edges in the initial mesh were used to partition the final geometry (Figure 5a). Some of these lines are necessarily geodesic because they belong to planes of symmetry. However, geodesic cutting lines were not necessarily sought for all seams. Due to the internal symmetries, it was possible to split the 3D surface into only three unique patterns depicted in Figures 5a. The patterning consisted of the following: 6x Pattern 1, 6x Pattern 2, and 6x Pattern 3 (Figure 5b-d). To reduce the deformations intrinsic to the flattening process, Pattern 1 was further divided into two symmetric halves. Pattern 2 took profit of the existence of three horizontal straight lines in a genus 2 Costa-Hoffman-Meeks surface.

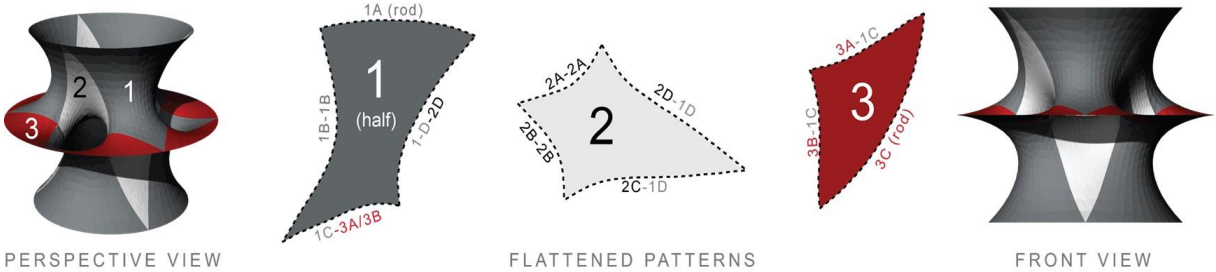

(a) (b) (c) (d) (e)

Figure 5: Final patterns of the 6-hole Costa surface

The 3D mesh of each pattern was flattened in Rhinoceros using the *Squish* command. This is a built-in algorithm that maps a non-developable 3D mesh into a 2D one (Rhinoceros 5, 2015). In principle, flattening should seek uniform deformations throughout the patterns. However, this is not possible for the chosen subdivision, especially for Patterns 1 and 2, since they present large negative Gaussian curvatures. The *Squish* settings were adjusted to generate a pattern that will undergo only stretching in the pullback process. The 3D geometry was considered as unstressed for the flattening process, so the final 2D patterns were scaled down by a uniform compensation factor of 20%, which was determined experimentally for the selected fabric (composed of 18% spandex, 82% nylon). Because of numerical imprecision during the flattening process, expected symmetries in individual patterns were not fully observed and had to be reimposed by averaging the relevant sides' lengths. Moreover, due to the fact that *Squish* considers each pattern independently during the flattening process, there was no guarantee that adjacent seam lines would have the same length between patterns. These differences were corrected through scaling factors, determined by using a least-squares method that minimized the absolute error between adjacent side lengths. The scaling factors for patterns 1, 2, and 3 were 1.032, 0.993, and 1.008, respectively.

3.2. Active-Bending Tensioning System

The model was designed with two primary tensioning systems: circular hoops for the three boundary conditions specified in the initial mesh, and a set of six bending-active rods to push apart the top and bottom rings, achieving a height of 1.5 meters as specified in the initial mesh. The pieces of the two tensioning systems are connected by 3D printed connectors.

Due to the membrane action, the lower and upper rings of the Costa surface sculpture will be subjected to opposing vertical forces (when disregarding self-weight, which is relatively small). If self-weight is disregarded, the loads applied to the middle ring by the membrane produce a zero resultant, but the weight of this ring introduces a slight increase in stresses acting in the upper half of the membrane, and a corresponding decrease in the stresses acting in its lower half.

The three circular rings act in compression and were built from straight fiberglass rod segments. The flexibility of these elements allowed them to be bent into shape in the elastic range, while their lightness was essential to minimize the stress variations imposed by the flexibility of the middle ring. Respecting the cyclic symmetry of the surface, the rings consisted of three segments connected by metal ferrules, inserted in custom-designed 3D printed connectors. Using three 1.57 m-long rods allowed for three junctions on each 1.5 m-diameter hoop, which coincided with the symmetries of the patterns and served as joints in which to insert the bending-active rods. The hoops are inserted in sleeves along the edges of the fabric that coincided with the boundary conditions.

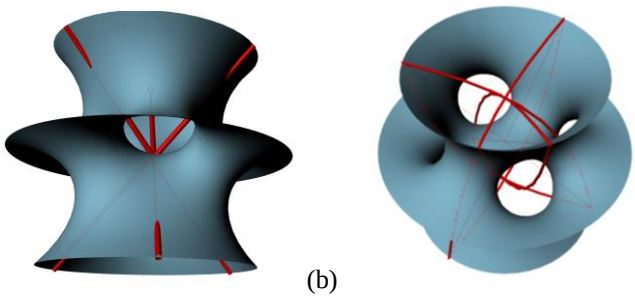

(a) (b)

Figure 6: (a) Three straight rods connecting the upper and lower rings along vertical planes of symmetry - each rod will intersect the surface in three points; (b) three pairs of buckled rods, each rod passing through the center of a hole, without intersecting the surface, with two common points of intersection

While the upper and lower rings could be pulled apart by a pair of external forces, a more elegant, self-equilibrated system can be achieved by joining these rings with members acting in compression. The initial concept envisioned connecting the rings with straight rods passing through the holes. However, the geometry of the surface does not allow a straight line to connect the upper and lower rings without intersecting the surface, as shown in Figure 6a. Therefore, the concept naturally evolved to a bending-active system, composed of three pairs of bent rods that push apart the upper and lower rings (Figure 6b). Such a solution required a precise determination of the deformed geometry and initial straight length of the rods, as well as custom 3D printed connectors. The shape of the bending-active rods was calculated following the model of the planar *elastica*, such that the rods pass through the center of the holes.

3.3. Manufacturing process

Once the final patterns were determined, a paper model of the surface was assembled using the patterns found as described in the previous section. The paper model served three important functions: first, it provided insight into the most efficient assembly sequence; second, it served as a map during the sewing process to keep track of the many different pieces of fabric (24 individual pieces' total); third, it provided a verification that gross errors were avoided in the patterning process.

A uniform seam allowance was added to interior edges, while a larger allowance was added to the naked edges to form sleeves to accommodate the three boundary rings. With these added details, the three final patterns were used to create tracing templates from MDF using a laser cutter. These templates allowed for systematic production of the 24 fabric pieces, which were finally sewn together according to the predefined sequence (Figure 7).

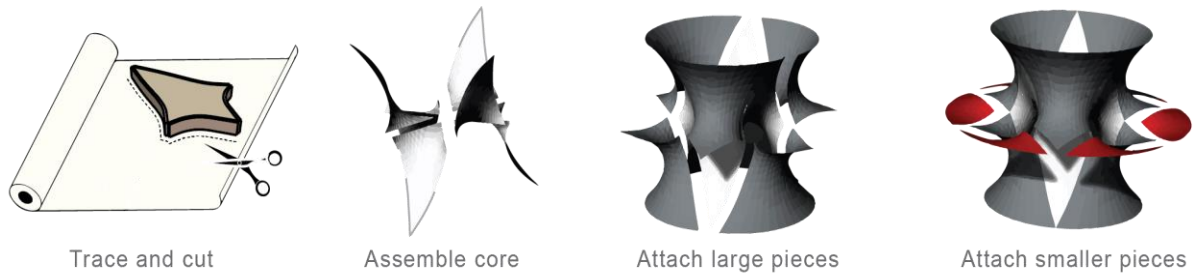

Figure 7: Assembly Sequence

Finally, the fiberglass rings were fabricated. 3D-printed four-way connectors were designed for the top and bottom rings to accept the buckled rods for the self-supporting mechanism. Once the rods were inserted into the fabric sleeves and bent into circles, the buckled rods were inserted into the connectors. Fully assembled, the surface showed no wrinkles and sat at a height of 1.5 meters as predicted by the computational model. It was necessary to tie the buckled rods together at their two ideal junctions to prevent out-of-plane buckling.

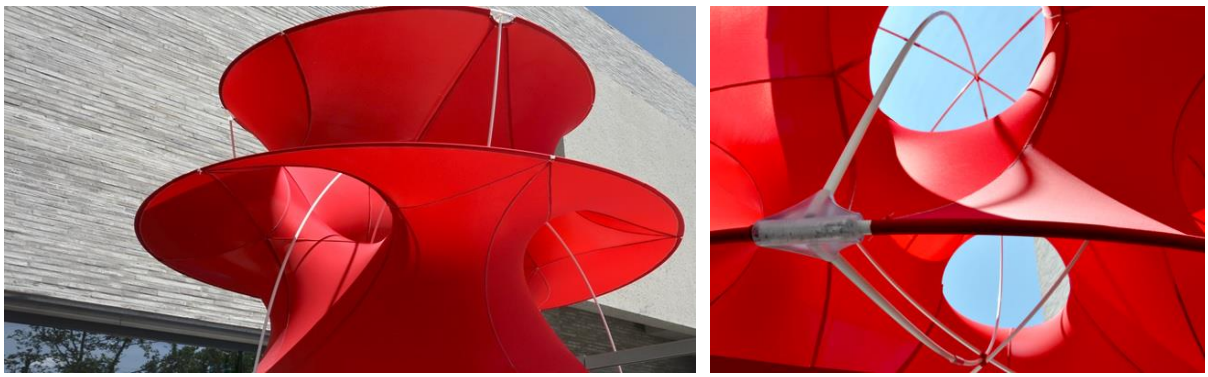

Figure 8: Assembled sculpture and close-up of connection details

4. Conclusions

The paper presented the design, analysis and fabrication of a membrane sculpture based on the Costa minimal surface, considering the use of an innovative bending-active support system, yielding a smooth and well-stretched fabric surface with remarkable adherence to the prescribed geometric parameters. The object required a sophisticated production and provided a successful academic example of interface between art, engineering and science.

Acknowledgements

R.M.O. Pauletti and S. Adriaenssens acknowledge the institutional support of the University of Princeton and the University of São Paulo. These authors were responsible for the proposition of the theme and provision of materials for the development of project. All design and production were conducted by co-authors A. Niewiarowski, V. Charpentier, M. Coar, T. Huynh and X. Li, which contributed equally to the redaction of the present article.

References

[1] Almgren, F. J. and J. E. Taylor (1976). "The geometry of soap films and soap bubbles." Scientific American 235: 82-93.

[2] Arcaro, V. F. and K. K. Klinka (2009). "Finite element analysis for geometrical shape minimization." Journal of the International Association for Shell and Spatial Structures 50(2): 79-86.

[3] Argyris, J. H., P. Dunne, T. Angelopoulos and B. Bichat (1974). "Large natural strains and some special difficulties due to non-linearity and incompressibility in finite elements." Computer Methods in Applied Mechanics and Engineering 4(2): 219-278.

[4] Barnes, M. (1975). Applications of dynamic relaxation to the design and analysis of cable, membrane and pneumatic structures. International Conference on Space Structures, Guildford.

[5] Costa, C. J. (1982). Imersões mínimas completas em R3 do gênero um e curvatura total finita, Conselho Nacional de Desenvolvimento Científico e Tecnológico, Instituto de Mathemática Pura e Aplicada.

[6] Cundall, P. (1976). "Explicit finite difference methods in geomechanics", Proceedings of E.F. Conference on Numerical Methods in Geomechanics, Blacksbourg, VA.

[7] Day, A. (1965). "An introduction to dynamic relaxation " The engineer 219: 218-221.

[8] Douglas, J. (1931). "Solution of the problem of Plateau." Transactions of the American Mathematical Society 33(1): 263-321.

[9] Eisenhart, L. P. (1909). A treatise on the differential geometry of curves and surfaces, Ginn.

[10] Hoffman, D. and W. H. Meeks (1990). "Embedded minimal surfaces of finite topology." Annals of Mathematics 131(1): 1-34.

[11] Hoffman, D. A. and W. Meeks III (1985). "A complete embedded minimal surface in R3 with genus one and three ends." Journal of differential geometry 21(1): 109-127.

[12] Isenberg, C. (1978). The science of soap films and soap bubbles, Courier Corporation.

[13] Linkwitz, K. (1971). New methods for the determination of cutting pattern of prestressed cable nets and their application to the Olympic Roofs Munich. Proceedings of the IASS pacific symposium on tension structures and space frames, Tokyo.

[14] Meeks III, W. and J. Pérez (2011). "The classical theory of minimal surfaces." Bulletin of the American Mathematical Society 48(3): 325-407.

[15] Otter, J. (1965). "Computations for prestressed concrete reactor pressure vessels using dynamic relaxation." Nuclear structural engineering 1(1): 61-75.

[16] Pauletti, R. (2006). An extension of the force density procedure to membrane structures. Proceedings of the IASS Symposium/APCS Conference–New Olympics, New Shell and Spacial Structures, Beijing.

[17] Pauletti, R. (2008). Static analysis of taut structures. Textile Composites and Inflatable Structures II, Springer: 117-139.

[18] Pauletti, R. M. and P. M. Pimenta (2008). "The natural force density method for the shape finding of taut structures." Computer Methods in Applied Mechanics and Engineering 197(49): 4419-4428.

[19] Pauletti, R. M. O. (2011). The Natural Force Density Method. IABSE-IASS Symposium - Taller, Longer, Lighter. London.

[20] Plateau, J. A. F. (1873). Statique expérimentale et théorique des liquides soumis aux seules forces moléculaires, Gauthier-Villars.

[21] Schek, H.-J. (1974). "The force density method for form finding and computation of general networks." Computer methods in applied mechanics and engineering 3(1): 115-134.

[22] Souza D.C.B. , Pauletti, R. M. O., Almeida N. E. S. (2008). Finding minimal surfaces by direct area minimization. IASS-SLTE International Symposium, Acapulco, 2008.